

Crystal Structure of Metallo DNA Duplex Containing Consecutive Watson–Crick-like T–Hg^{II}–T Base Pairs**

Jiro Kondo,* Tom Yamada, Chika Hirose, Itaru Okamoto, Yoshiyuki Tanaka, and Akira Ono

Abstract: The metallo DNA duplex containing mercury-mediated T–T base pairs is an attractive biomacromolecular nanomaterial which can be applied to nanodevices such as ion sensors. Reported herein is the first crystal structure of a B-form DNA duplex containing two consecutive T–Hg^{II}–T base pairs. The Hg^{II} ion occupies the center between two T residues. The N3–Hg^{II} bond distance is 2.0 Å. The relatively short Hg^{II}–Hg^{II} distance (3.3 Å) observed in consecutive T–Hg^{II}–T base pairs suggests that the metalphilic attraction could exist between them and may stabilize the B-form double helix. To support this, the DNA duplex is largely distorted and adopts an unusual nonhelical conformation in the absence of Hg^{II}. The structure of the metallo DNA duplex itself and the Hg^{II}-induced structural switching from the nonhelical form to the B-form provide the basis for structure-based design of metal-conjugated nucleic acid nanomaterials.

The DNA molecule is an attractive material in pharmaceutical technology and nanotechnology because of its chemical stability, ease of chemical synthesis and sequence design, and relatively simple structure resulting from base complementarity. For example, the antigene and antisense DNAs, deoxyribozymes, and DNA aptamers have been extensively developed as nucleic acid medicines and biotechnological tools.^[1] Recent discoveries and extensive studies of metal-mediated pairs of natural and artificial bases expand considerably the design possibility of functional DNA molecules.^[2] The metal-mediated base pairs have been applied to DNA

molecular devices, such as ion sensors,^[3] electric transport nanowires,^[4] and DNA magnets.^[5] However, only some structural information of nucleic acid duplexes containing metal-mediated base pairs are available.^[6]

The mercury-mediated T–T base pair (T–Hg^{II}–T) has been investigated for more than fifty years.^[7] In our recent study, we observed that Hg^{II} significantly stabilizes a DNA duplex by binding selectively to a T–T mispair.^[8] Based on the phenomenon observed, we developed a DNA-based sensing system which selectively and sensitively detects Hg^{II} in aqueous solution.^[3a] The Hg^{II} binding mode in the T–Hg^{II}–T base pair was determined in solution both with ¹⁵N NMR and Raman spectroscopy.^[9] The binding of Hg^{II} was also observed in the pioneering crystallographic study of a 2:1 complex of 1-methylthymine/Hg^{II}.^[10] However, structural information of a metallo DNA duplex containing the T–Hg^{II}–T base pair is missing, even though structures of some artificial DNA duplexes containing metal-mediated base pairs have been studied.^[5a,c,6d–f] Very recently, we have successfully solved the solution structure of a DNA duplex containing two consecutive T–Hg^{II}–T base pairs by using NMR spectroscopy.^[11] In the present study, we have performed the X-ray analysis of a DNA duplex both in the presence and absence of Hg^{II} to obtain more detailed structural information and to unveil the effect of Hg^{II} binding on the whole structure of the DNA duplex. The data acquired in crystalline and solution states provide a reliable structural basis for advanced design and further development of metallo DNAs.

The DNA dodecamer d(CGCGATTTTCGCG), 12TT hereafter, was designed to fold as a self-complementary duplex containing tandem T–T mismatches at the center. Such DNA fragments have been extensively used as successful models in the crystallographic studies of B-form DNAs containing natural and modified bases.^[12] For phase determination by the multiple anomalous diffraction (MAD) method, the DNA dodecamer containing 5-bromocytosine at the third position, 12TT-Br hereafter, was also synthesized. Crystals were obtained both in the presence and absence of Hg^{II} (Table 1). Crystal structures of DNA duplexes with and without Hg^{II}, 12TT/Hg^{II}, 12TT, and 12TT-Br hereafter, have been deposited in the Protein Data Bank (PDB) with the ID codes 4L24, 4L25, and 4L26, respectively. A detailed description of materials and methods of this study is included in Supporting Information.

In the presence of Hg^{II} (12TT/Hg^{II} crystal in Table 1), two DNA strands form an antiparallel right-handed double helix (Figure 1). At both ends of the double helix, canonical Watson–Crick G–C and A–T base pairs are formed (base pairs are named according to the Leontis/Westhof classification).^[13] In the central part of the double helix, two Hg^{II} ions bridge the

[*] Dr. J. Kondo, T. Yamada, C. Hirose
Department of Materials and Life Sciences, Faculty of Science and Technology, Sophia University
7-1 Kioi-cho, Chiyoda-ku, 102-8554 Tokyo (Japan)
E-mail: j.kondo@sophia.ac.jp

Dr. I. Okamoto, Prof. A. Ono
Department of Material and Life Chemistry, Faculty of Engineering, Kanagawa University, Yokohama 221-8686 (Japan)

Dr. Y. Tanaka
Laboratory of Molecular Transformation, Graduate School of Pharmaceutical Sciences, Tohoku University
Sendai 980-8578 (Japan)

[**] This work was supported by a Grant-in-Aid for Scientific Research (A) (No. 24245037), and in part by a Strategic Research Foundation Grant-aided Project for Private Universities (No. S1201015) from the Ministry of Education, Culture, Sports, Science and Technology (Japan) (MEXT). We thank the Photon Factory for provision of synchrotron radiation facilities (No. 2011G630) and acknowledge the staff of the BL-1A and NW12A beamlines. We are grateful to Dr. V. Sychrovský and Prof. E. Westhof for helpful discussions and critical reading of the manuscript.

Supporting information for this article is available on the WWW under <http://dx.doi.org/10.1002/anie.201309066>.

Table 1: Crystal data, statistics of data collections, and structure refinements.

	12TT/Hg ^{II}	12TT	12TT-Br
Crystal data			
Space group	<i>P</i> 2 ₁ 2 ₁ 2 ₁	<i>P</i> 2 ₁	<i>P</i> 2 ₁
Unit cell (Å, °)	<i>a</i> = 25.5, <i>b</i> = 41.3, <i>c</i> = 64.6	<i>a</i> = 27.3, <i>b</i> = 39.3, <i>c</i> = 30.7 <i>β</i> = 98.3	<i>a</i> = 27.4, <i>b</i> = 39.3, <i>c</i> = 30.5 <i>β</i> = 99.4
<i>Z</i> ^[a]	1	1	1
Data collection			
Beamline	BL-1A of PF	BL-1A of PF	NW12A of PF*
Wavelength (Å)	1.0	1.0	0.91942/0.92006/1.0
Resolution (Å)	34.8–2.7	19.1–1.1	30.1–1.5/22.0–1.4/21.9–1.4
of the outer shell (Å)	2.8–2.7	1.14–1.1	1.6–1.5/1.5–1.4/1.5–1.4
Unique reflections	2064	24441	10050/12392/12212
Completeness (%)	99.3	93.2	96.8/94.9/94.9
in the outer shell (%)	100.0	91.7	98.9/96.4/95.4
<i>R</i> _{merge} ^[b] (%)	7.3	3.7	–
in the outer shell (%)	32.3	16.5	–
<i>R</i> _{anom} ^[c] (%)	–	–	7.3/6.8/6.1
in the outer shell (%)	–	–	26.2/34.6/30.4
Redundancy	6.4	3.7	3.6/1.8/1.8
in the outer shell	6.8	3.8	3.7/1.8/1.8
Structure refinement			
Resolution range (Å)	34.8–2.7	19.1–1.1	21.9–1.4
Used reflections	2064	24438	12212
<i>R</i> -factor ^[d] (%)	25.8	23.1	23.2
<i>R</i> _{free} ^[e] (%)	26.7	24.1	26.6
RNA atoms	484	484	486
Hg ^{II} ions	2	–	–
Water molecules	14	170	135
R.m.s.d. bond length (Å)	0.006	0.003	0.003
R.m.s.d. bond angles (°)	1.3	0.9	1.0

[a] Number of DNA duplex in the asymmetric unit. [b] $R_{\text{merge}} = 100 \times \sum_{hklj} |I_{hklj} - \langle I_{hklj} \rangle| / \sum_{hklj} \langle I_{hklj} \rangle$. [c] $R_{\text{anom}} = 100 \times \sum_{hklj} |I_{hklj}(+) - I_{hklj}(-)| / \sum_{hklj} [I_{hklj}(+) + I_{hklj}(-)]$. [d] $R\text{-factor} = 100 \times \sum |F_o| - |F_c| / \sum |F_o|$, where $|F_o|$ and $|F_c|$ are optimally scaled observed and calculated structure factor amplitudes, respectively. [e] Calculated using a random set containing 10% of observations. * For phase determination with the multiple anomalous diffraction (MAD) method, three datasets were collected with three wavelengths. Statistics from left to right are of peak, edge, and remote data, respectively.

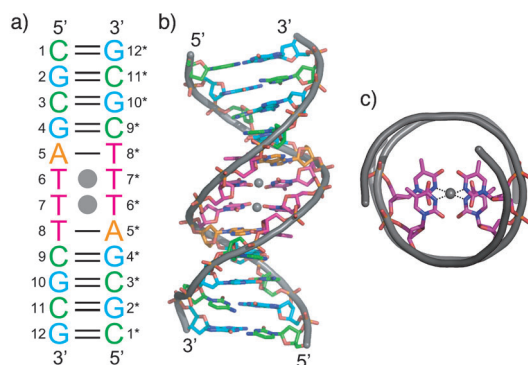


Figure 1. a) Secondary structure and b,c) crystal structure (side view and top view, respectively) of the B-form DNA duplex obtained in the presence of Hg^{II}. In these figures, Hg^{II} ions are shown as gray spheres. In (c), only two T-Hg^{II}-T base pairs are shown, and covalent bonds between N3 of T and Hg^{II} are represented by dashed lines.

T bases of the T-T mispairs, thereby forming consecutive T-Hg^{II}-T base pairs with very similar geometries to that of Watson-Crick pairs. The local helical parameters, intra-base-pair parameters, and pseudorotation phase angles clearly indicate that the DNA duplex adopts the standard B-form conformation (Tables S2 and S3). A superimposition of the

metallo DNA duplex onto the normal B-form DNA duplex with two Watson-Crick A-T base pairs instead of the T-Hg^{II}-T pairs at the center (PDB-ID 1BNA)^[12a] shows the root-mean-square deviation to be 0.7 Å (see Figure S1 in the Supporting Information), thus indicating that the formation of the Hg^{II}-mediated T-T base pairs causes no significant changes in the overall B-form DNA conformation.

The electron density maps and geometries of the T-Hg^{II}-T base pairs are shown in Figure 2. As is clear from the shape of $2|F_o| - |F_c|$ map, opposite T residues do not form the possible wobble-type T-T base pair through two hydrogen bonds O2...H-N3 and N3-H...O4. While the $2|F_o| - |F_c|$ maps for the Watson-Crick G-C and A-T base pairs are very sharp (see Figure S2), those for the T-Hg^{II}-T pairs are broadened at the center, where the Hg^{II} ion exists. It is clear from the omit map calculated after removing two Hg^{II} ions that the metal ion occupies the center between two T residues. The distance between the N3 atom of T and the Hg^{II} ion is 2.0 Å. The N3 atom releases an imino proton even at neutral pH (*pK_a* value of N3 position of T is 9.8)^[14] and directly bonds to Hg^{II}. The N3-Hg^{II}-N3 bond is linear and the N-N distance is 4.0 Å. The local geometry of metal linkage in the T-Hg^{II}-T base pairs are basically identical to that observed in the crystal of a 2:1 complex of 1-methylthymine/Hg^{II} and our theoretical

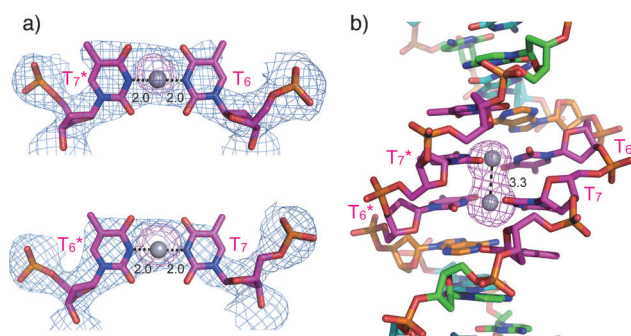


Figure 2. a) Local $2|F_o| - |F_c|$ (blue: 1σ contour level) and omit (magenta: 6σ contour level) maps for T-Hg^{II}-T base pairs. b) Side view of local omit map (magenta: 6σ contour level) for Hg^{II} ions. In these figures, Hg^{II} ions are shown as gray spheres. Distances (Å) between N3 of T and Hg^{II} and between two Hg^{II} ions are represented by dashed lines.

calculations, in which the N3-Hg^{II} distances are 2.04 Å and 2.07–2.15 Å, respectively.^[10,15] The propeller twist angles of the T-Hg^{II}-T base pairs (-22° and -20°) are remarkably larger than that of the canonical Watson–Crick base pairs in the B-form DNA (-1° ; see Figure 2b and Table S2). The propeller twist occurs probably because there is no extra bond except the N3-Hg^{II}-N3 bonds between two T residues, and because of the repulsion of carbonyl groups. The electron densities of the T residues are relatively poorly resolved at position C5 (Figure 2a), and may be ascribed to the mobility of the T residues mainly around the propeller axis. Although the C1'-C1' distances of the T-Hg^{II}-T base pairs (9.5–9.6 Å) are 1 Å shorter than those in the canonical Watson–Crick base pairs (ca. 10.7 Å), the B-form conformation of the metallo DNA duplex is not distorted (see Table S2). The normal structural appearance of DNA containing the T-Hg^{II}-T base pairs probably explains the fact that DNA polymerase incorporated dTTP against T residues of the template DNA strand in the presence of Hg^{II}.^[16]

In the B-form DNA, the helical axis runs through the center of the base pairs, and the Hg^{II} ions in the mercury-mediated base pairs are therefore aligned along the helical axis (Figure 1c). The distance between the two Hg^{II} atoms is 3.3 Å (Figure 2b). The relatively short distance between the two Hg^{II} cations indicates that the duplex stabilization may be due to mercury–mercury metallophilic attraction^[17] which was suggested in our previous computational and spectroscopic studies.^[15a,b] A similar observation has recently been reported for the NMR solution structure of a B-form DNA duplex containing three consecutive imidazole–Ag^I–imidazole base pairs,^[6d,e] in which the average Ag^I–Ag^I distance is 3.45 Å.

Our solution structure of a DNA decamer duplex containing two consecutive T-Hg^{II}-T base pairs, which will be reported elsewhere,^[11] has very similar features to the present crystal structure (see Tables S4 and S5 and Figure S3). In the solution structure, however, the T-Hg^{II}-T base pair geometry was constrained based on the crystal structure of the 2:1 complex of 1-methylthymine/Hg^{II},^[10] and the Hg^{II}-Hg^{II} distance, derived solely with NMR data, was about 4 Å.

Therefore, the precise geometrical information of the T-Hg^{II}-T base pair and the Hg^{II}-Hg^{II} distance in the B-form DNA duplex have first been determined at the atomic level by the present X-ray analysis.

In the absence of Hg^{II} (12TT and 12TT-Br crystals in Table 1), the DNA duplex adopts an unusual nonhelical conformation (Figure 3), which is totally different from the B-

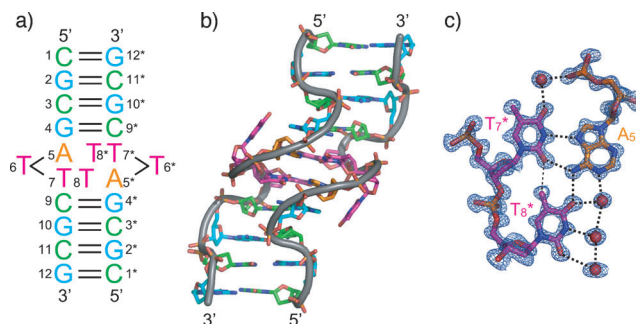


Figure 3. a) Secondary structure and b) crystal structure of the non-helical DNA duplex obtained in the absence of Hg^{II}, and c) local $2|F_o| - |F_c|$ map for an A₅-T₇*-T₈* triplet in the DNA duplex contoured at 1σ level. Hydrogen bonds and a C-H...O interaction are represented by thick and thin dashed lines, respectively. Oxygen atoms of water molecules are shown as red spheres.

form double helix observed in the presence of Hg^{II}. The duplex terminal parts consisting of four Watson–Crick G-C base pairs take a left-handed twist conformation corresponding to so-called Z-form. The G residues in G-C pairs adopt *syn* conformation around the glycosyl bond. The central part of the duplex adopts a right-handed helical form. The whole DNA molecule can be therefore characterized as a nonhelical structure with notably distorted central part. The A₅ residue does not form the Watson–Crick base pair with the opposite T₈* residue, but forms an A₅-T₇*-T₈* triplet (Figure 3c). In the triplet, the following three hydrogen bonds and a weak C-H...O interaction are observed: N7(A₅)...H-N3(T₇*), N6(A₅)-H...O2(T₇*), N6(A₅)-H...O4(T₈*), and O2(T₇*)...H-C5(T₈*). The geometry of the adjacent thymine residues T₇pT₈ is identical to the dinucleotide platform motif found in several RNA molecules.^[18] The T₆ residue bulges out from the duplex and makes no intramolecular hydrogen bond. In a previously observed left-handed to right-handed transition, the left-handed Z-form conformation has to be stabilized by a Z-DNA binding protein.^[19] In contrast, the DNA fragment used in this study does not require such a protein to keep its nonhelical conformation. The structure obtained in the absence of Hg^{II} confirms the view that Hg^{II} ions are necessary for the DNA duplex to maintain the B-form conformation, due not only to the T-Hg^{II}-T base-pair formation but also to the stabilization through the metallophilic attraction of the consecutive Hg^{II} ions.

In conclusion, the crystal structures of the DNA duplexes solved both in the presence and absence of Hg^{II} revealed the following: a) the tandem T-T mismatches largely distort DNA double helix, b) Hg^{II} ions particularly stabilize the B-form conformation by forming the T-Hg^{II}-T base pairs, c) the

mercury-mediated base pair is structurally similar to the normal Watson–Crick base pairs in regard to its size and position within DNA duplex, d) the relatively short mercury–mercury distance observed inside DNA is suggestive of the stabilizing metallophilic attraction between Hg^{II} ions in consecutive T– Hg^{II} –T base pairs. The first crystal structure of the metallo DNA duplex consisting exclusively of natural DNA bases provides the necessary basis for structure-based design of metal-conjugated nucleic acid nanomaterials. In addition, the Hg^{II} -induced structural change from the non-helical form to the B-form can be applicable to nanoscale switching devices.

Received: October 17, 2013

Revised: December 6, 2013

Published online: January 29, 2014

Keywords: DNA · helical structures · mercury · metalation · structure elucidation

- [1] a) L. M. Alvarez-Salas, *Curr. Top. Med. Chem.* **2008**, *8*, 1379–1404; b) G. F. Delevey, M. J. Damha, *Chem. Biol.* **2012**, *19*, 937–954; c) S. Schubert, J. Kurreck, *Curr. Drug. Targets* **2004**, *5*, 667–681; d) C. Höbartner, S. K. Silverman, *Biopolymers* **2007**, *87*, 279–292; e) H. Xing, N. Y. Wong, Y. Xiang, Y. Lu, *Curr. Opin. Chem. Biol.* **2012**, *16*, 429–435.
- [2] a) H. A. Wagenknecht, *Angew. Chem.* **2004**, *116*, 3322–3324; *Angew. Chem. Int. Ed.* **2003**, *42*, 3204–3206; b) G. H. Clever, C. Kaul, T. Carell, *Angew. Chem.* **2007**, *119*, 6340–6350; *Angew. Chem. Int. Ed.* **2007**, *46*, 6226–6236; c) Y. Takezawa, M. Shionoya, *Acc. Chem. Res.* **2012**, *45*, 2066–2076; d) P. Scharf, J. Müller, *ChemPlusChem* **2013**, *78*, 20–34.
- [3] a) A. Ono, H. Togashi, *Angew. Chem.* **2004**, *116*, 4400–4402; *Angew. Chem. Int. Ed.* **2004**, *43*, 4300–4302; b) A. Ono, S. Cao, H. Togashi, M. Tashiro, T. Fujimoto, T. Machinami, S. Oda, Y. Miyake, I. Okamoto, Y. Tanaka, *Chem. Commun.* **2008**, 4825–4827; c) E. M. Nolan, S. J. Lippard, *Chem. Rev.* **2008**, *108*, 3443–3480; d) D. L. Ma, D. S. Chan, B. Y. Man, C. H. Leung, *Chem. Asian J.* **2011**, *6*, 986–1003; e) Y. Song, W. Wei, X. Qu, *Adv. Mater.* **2011**, *23*, 4215–4236.
- [4] a) T. Carell, C. Behrens, J. Gierlich, *Org. Biomol. Chem.* **2003**, *1*, 2221–2228; b) T. Ito, G. Nikaïdo, S. I. Nishimoto, *J. Inorg. Biochem.* **2007**, *101*, 1090–1093; c) J. Joseph, G. B. Schuster, *Org. Lett.* **2007**, *9*, 1843–1846; d) L. Q. Guo, N. Yin, G. N. Chen, *J. Phys. Chem. C* **2011**, *115*, 4837–4842; e) H. Isobe, N. Yamazaki, A. Asano, T. Fujino, W. Nakanishi, S. Seki, *Chem. Lett.* **2011**, *40*, 318–319; f) S. Liu, G. H. Clever, Y. Takezawa, M. Kaneko, K. Tanaka, X. Guo, M. Shionoya, *Angew. Chem.* **2011**, *123*, 9048–9052; *Angew. Chem. Int. Ed.* **2011**, *50*, 8886–8890.
- [5] a) K. Tanaka, A. Tengeiji, T. Kato, N. Toyama, M. Shionoya, *Science* **2003**, *299*, 1212–1213; b) S. S. Mallajosyula, S. K. Pati, *Angew. Chem.* **2009**, *121*, 5077–5081; *Angew. Chem. Int. Ed.* **2009**, *48*, 4977–4981; c) G. H. Clever, S. J. Reitmeier, T. Carell, O. Schiemann, *Angew. Chem.* **2010**, *122*, 5047–5049; *Angew. Chem. Int. Ed.* **2010**, *49*, 4927–4929.
- [6] a) S. Atwell, E. Meggers, G. Spraggon, P. G. Schultz, *J. Am. Chem. Soc.* **2001**, *123*, 12364–12367; b) E. Ennifar, P. Walter, P. Dumas, *Nucleic Acids Res.* **2003**, *31*, 2671–2682; c) M. K. Schlegel, L. O. Essen, E. Meggers, *J. Am. Chem. Soc.* **2008**, *130*, 8158–8159; d) S. Johannsen, N. Megger, D. Böhme, R. K. O. Sigel, J. Müller, *Nat. Chem.* **2010**, *2*, 229–234; e) S. Kumbhar, S. Johannsen, R. K. O. Sigel, M. P. Waller, J. Müller, *J. Inorg. Biochem.* **2013**, *127*, 203–210; f) C. Kaul, M. Müller, M. Wagner, S. Schneider, T. Carell, *Nat. Chem.* **2011**, *3*, 794–800.
- [7] a) S. Katz, *Nature* **1962**, *195*, 997–998; b) S. Katz, *Biochim. Biophys. Acta.* **1963**, *68*, 240–253; c) Z. Kuklenyik, L. G. Marzilli, *Inorg. Chem.* **1996**, *35*, 5654–5662.
- [8] Y. Miyake, H. Togashi, M. Tashiro, H. Yamaguchi, S. Oda, M. Kudo, Y. Tanaka, Y. Kondo, R. Sawa, T. Fujimoto, T. Machinami, A. Ono, *J. Am. Chem. Soc.* **2006**, *128*, 2172–2173.
- [9] a) Y. Tanaka, S. Oda, H. Yamaguchi, Y. Kondo, C. Kojima, A. Ono, *J. Am. Chem. Soc.* **2007**, *129*, 244–245; b) Y. Tanaka, A. Ono, *Dalton Trans.* **2008**, 4965–4974; c) T. Uchiyama, T. Miura, H. Takeuchi, T. Dairaku, T. Komuro, T. Kawamura, Y. Kondo, L. Benda, V. Sychrovský, P. Bouř, I. Okamoto, A. Ono, Y. Tanaka, *Nucleic Acids Res.* **2012**, *40*, 5766–5774.
- [10] L. D. Kosturko, C. Folzer, R. F. Stewart, *Biochemistry* **1974**, *13*, 3949–3952.
- [11] H. Yamaguchi, J. Šebera, J. Kondo, S. Oda, T. Komuro, T. Kawamura, T. Daraku, Y. Kondo, I. Okamoto, A. Ono, J. V. Burda, C. Kojima, V. Sychrovský, Y. Tanaka, *Nucleic Acids Res.*, DOI: 10.1093/nar/gkt1344.
- [12] a) H. R. Drew, R. M. Wing, T. Takano, C. Broka, S. Tanaka, K. Itakura, R. E. Dickerson, *Proc. Natl. Acad. Sci. USA* **1981**, *78*, 2179–2183; b) E. C. Juan, J. Kondo, T. Kurihara, T. Ito, Y. Ueno, A. Matsuda, A. Takénaka, *Nucleic Acids Res.* **2007**, *35*, 1969–1977.
- [13] a) N. B. Leontis, E. Westhof, *RNA* **2001**, *7*, 499–512; b) N. B. Leontis, J. Stombaugh, E. Westhof, *Nucleic Acids Res.* **2002**, *30*, 3497–3531.
- [14] W. Saenger, *Principles of Nucleic Acid Structure*, Springer, New York, **1984**.
- [15] a) L. Benda, M. Straka, Y. Tanaka, V. Sychrovský, *Phys. Chem. Chem. Phys.* **2011**, *13*, 100–103; b) L. Benda, M. Straka, V. Sychrovský, P. Bouř, Y. Tanaka, *J. Phys. Chem. A* **2012**, *116*, 8313–8320; c) J. Šebera, J. Burda, M. Straka, A. Ono, C. Kojima, Y. Tanaka, V. Sychrovský, *Chem. Eur. J.* **2013**, *19*, 9884–9894.
- [16] H. Urata, E. Yamaguchi, T. Funai, Y. Matsumura, S. Wada, *Angew. Chem.* **2010**, *122*, 6666–6669; *Angew. Chem. Int. Ed.* **2010**, *49*, 6516–6519.
- [17] a) P. Pyykkö, *Chem. Rev.* **1997**, *97*, 597–636; b) P. Pyykkö, M. Straka, *Phys. Chem. Chem. Phys.* **2000**, *2*, 2489–2493.
- [18] a) J. H. Cate, A. R. Gooding, E. Podell, K. Zhou, B. L. Golden, C. E. Kundrot, T. R. Cech, J. A. Doudna, *Science* **1996**, *273*, 1678–1685; b) J. H. Cate, A. R. Gooding, E. Podell, K. Zhou, B. L. Golden, A. A. Szewczak, C. E. Kundrot, T. R. Cech, J. A. Doudna, *Science* **1996**, *273*, 1696–1699; c) X. L. Lu, W. K. Olson, H. J. Bussemaker, *Nucleic Acids Res.* **2010**, *38*, 4868–4876.
- [19] S. C. Ha, K. Lowenhaupt, A. Rich, Y. G. Kim, K. K. Kim, *Nature* **2005**, *437*, 1183–1186.